Journal of Physics: Conference Series **246** (2010) 012035 doi:10.1088/1742-6596/246/1/012035

Catastrophic shifts in ecosystems: spatial early warnings and management procedures (Inspired in the physics of phase transitions)

H Fort[1], N Mazzeo[2], M Scheffer[3] and E van Nes[3]

[1] Complex Systems Group, Instituto de Física, Facultad de Ciencias, Universidad de la República, Iguá 4225, 11400 Montevideo, Uruguay
[2] Depto. de Ecología, Facultad de Ciencias, Universidad de la República, Iguá 4225, 11400 Montevideo, Uruguay
[3] Wageningen Agricultural University, Aquatic Ecology and Water Quality Management Group, PO Box 47, 6700 AA Wageningen, The Netherlands

E-mail: hugo@fisica.edu.uy

Abstract. Ecosystems are complex systems which can respond to gradual changes of their conditions by a sudden shift to a contrasting regime or alternative stable state (ASS). Predicting such critical points before they are reached is extremely difficult and providing early warnings is fundamental to design management protocols for ecosystems. Here we study different spatial versions of popular ecological models which are known to exhibit ASS. The spatial heterogeneity is introduced by a local parameter varying from cell to cell in a regular lattice. Transport of biomass among cells occurs by simple diffusion. We investigate whether different quantities from statistical mechanics -like the variance, the two-point correlation function and the patchiness- may serve as early warnings of catastrophic phase transitions between the ASS. In particular, we find that the patch-size distribution follows a power law when the system is close to the catastrophic transition. We also provide links between spatial and temporal indicators and analyze how the interplay between diffusion and spatial heterogeneity may affect the earliness of each of the observables. Finally, we comment on similarities and differences between these catastrophic shifts and paradigmatic thermodynamic phase transitions like the liquid-vapor change of state for a fluid like water.

1. Catastrophic Shifts in Ecosystems

Several ecosystems are known to display sudden catastrophic regime shifts when exposed to gradual change in external conditions such as climate, inputs of nutrients, toxic chemicals, etc. Recent examples illustrating such changes are the shift in Caribbean coral reefs [1, 2], shallow lakes that become overgrown by floating plants [3], savannahs that have been suddenly encroached by bushes [4, 5] and lakes that shift from clear to turbid [6, 7]. Such drastic shifts occur because the ecosystem has alternative stable states (ASS) [8, 9]. In other words, under the same external conditions the system can be in two or more stable states. Hence, when subjected to a slowly changing external factor, an ecosystem may show little change until at a critical point where a sudden transition between two different ASS occurs. The presence of ASS implies hysteresis, *i.e.* once a system has gone through a state shift, it tends to remain in the new state until the control variable is changed back to a much lower or higher level.

1.1. The Search of Spatial Early Warnings

The simplest models to describe alternative states in ecosystems are *mean-field* (MF) models. Neglecting all spatial heterogeneities, these models describe the change over time of some population that characterizes the state of the ecosystem. These models are easy to analyse and in cases without significant heterogeneity their predictions are not very different from those of spatial models. However, in other cases the presence of a spatial dimension profoundly alters population dynamics or opportunities for coexistence in the real world [10]. In fact, the oversimplification of MF models casts doubt on whether the occurrence of an alternative stable state could be an artefact. Moreover, verifications and predictive power with respect to catastrophic responses to a changing environmental conditions are still scarce for spatially extensive ecosystems. Analysis of spatially explicit models are relevant, for example, to understand phenomena like clumping and spatial segregation in plant communities [11]. It was shown that vegetation patches, which have been extensively studied for arid lands [12], can be approached as a pattern formation phenomenon [13]-[14]. It has been hypothesized that vegetation patchiness could be used as a signature of imminent catastrophic shifts between alternative states [15]. Evidences that the patch-size distribution of vegetation follows a power law were later found in arid Mediterranean ecosystems [16]. This implies that vegetation patches were present over a wide range of size scales, thus displaying scale invariance. It was also found that with increasing grazing pressure, the field data revealed deviations from power laws. Hence, the authors proposed that this power law behaviour may be a warning signal for the onset of desertification. These spatial *early warnings* complement temporal ones like the variance of time series introduced to detect lake eutrophication [17]. [Eutrophication is an increase in nutrients leading to an enhanced growth of aquatic vegetation or phytoplankton and further effects including lack of oxygen and severe reductions in water quality, fish, and other animal populations.]

1.2. Preventive Actions and Management Protocols

Once you have early warnings of an undesired catastrophic shifts, the next step is to implement preventive actions to avoid such transitions.

For instance, an example of catastrophic shift is the desertification of arid lands produced by over-grazing. Management of grazing pressure (either by stock or native species or pests) is crucial to prevent environmental degradation and to combat desertification. We will illustrate this by considering the effects of a simple remedial action in a *grazing model*.

Often the interests of different ecosystem users are in conflict. This is illustrated with lake management of aquatic vegetation. Nature conservationists prefer a dense vegetation because it promotes biodiversity and avoids potentially toxic agents like cyanobacteria. On the other hand, recreational users (boaters, surfers, swimmers) are hindered by aquatic plants. To consider the interests of all users, harvesting strategies that keep an intermediate level of submerged biomass might be a possible solution. Hence we will address the problem of lakes that shift among different primary producers dominance (phytoplankton, submerged or floating plants) through a another model, a *harvesting model* for submerged plants.

2. Spatial Ecological Models

2.1. Mean-Field Models

In this work we will consider the spatial version of some popular ecological models in terms of just a single-species biomass density which grows logistically and whose consumption, loss or removal (either by grazing, predation or harvesting) is represented by a saturation curve of Holling type II or III [18].

Both these models, in terms of two parameters, are known to have ASS.

2.1.1. First Example: Grazing Model A population model initially introduced to describe grazing systems [19], and later used in general for several ecosystems [20] and in particular for the case of the spruce budworm [21, 22], involves a Holling type III consumption term. The corresponding dynamical equation, in terms of all non-dimensional quantities, can be written as:

$$\frac{dX}{dt} = X\left(1 - \frac{X}{K}\right) - c\frac{X^2}{1+X^2}, \tag{1}$$

where X corresponds to the biomass density, K to the carrying capacity, or the number of individuals which can be supported in a given area within natural resource limits, and c to the maximum consumption rate.

The r.h.s. of (1) may be thought as the gradient of a potential V_g :

$$V_g = -\int dX\left[X\left(1 - \frac{X}{K}\right) - c\frac{X^2}{1+X^2}\right] = -\frac{X^2}{2} + \frac{X^3}{3K} + c\left(X - \arctan X\right), \tag{2}$$

so the equilibria or attractors correspond to the roots of the first derivative of V_g.

2.1.2. Second Example: Harvesting Model for Submerged Plants The harvesting of submerged plants in lakes can be modelled by a Holling type II consumption term [23]. So, again in terms of non-dimensional quantities, X evolves according to

$$\frac{dX}{dt} = X\left(1 - \frac{X}{K}\right) - c\frac{X}{1+X}. \tag{3}$$

In complete analogy with the grazing model, the associated potential is given by: $V_h = -\frac{X^2}{2} + \frac{X^3}{3K} + c\left(X - \ln(1+X)\right)$.

2.2. Cellular Automata

In order to take into account the spatial heterogeneity of the landscape one of the two parameters, the *local* parameter, is taken as dependent on the position. The other parameter, the *global* parameter, is taken uniform in all the system.

A two dimensional spatial version of the previous mean-field models is given by:

$$\frac{dX(x,y;t)}{dt} = X\left(1 - \frac{X(x,y;t)}{K(x,y)}\right) - c\frac{X(x,y;t)^q}{1+X(x,y;t)^q} + D\nabla^2 X(x,y;t) \tag{4}$$

where the carrying capacity $K(x,y)$ is a spatial heterogeneous parameter that varies from point to point (while the parameter c is taken as uniform), the exponent q is equal to 1 (2) for the harvesting (grazing) model and D is the diffusion coefficient measuring dispersion of X in space. We simulated these models in a $L \times L$ regular square lattice, so each cell, centred at integer coordinates (i,j), can be associated with a patch of the ecosystem. Each cell is connected to its four nearest neighbours *i.e.* the von Neumann neighbourhood is used. In other words, we get a cellular automaton whose update rule is given by:

$$\begin{aligned} X(i,j;t+1) = X(i,j,t) + X(i,j;t)\left(1 - \frac{X(i,j;t)}{K(i,j)}\right) - c\frac{X(i,j;t)^q}{1+X(i,j;t)^q} + \\ d[X(i+1,j;t) + X(i-1,j;t) + X(i,j+1;t) + X(i,j-1;t) - 4X(i,j;t)], \end{aligned} \tag{5}$$

where d is a reduced diffusion coefficient related with D and the lattice spacing a by $d = 4D/a^2$. Periodic boundary conditions (PBC) were used and L ranged from 100 to 800 (in fact, for different values of L in this range, no important differences were found). The number of time

steps is typically 1000. Depending on the ecosystem, each time step could correspond to a day, or a month, or a year, etc.

The range of values for the model parameters that we use are chosen to contain the region of alternative stable states determined by the MF equations: the carrying capacity $K(i,j)$ varies randomly from cell to cell around a fixed spatial mean $\langle K\rangle$ (a typical value for this average is 7.5) in the interval $[-\delta_K, \delta_K]$ where $\delta_K = 1.0 - 2.5$. Typical values for the consumption rate c are between 1 and 3 and for for d are between 0.1 and 5.

2.3. Observables

Several quantities can be measured:

- The *spatial mean* $\langle X\rangle$:
$$\langle X\rangle(t) = \frac{1}{L^2}\sum_{i,j} X(i,j,t) \tag{6}$$
(i and j locate each cell of the array).
- The *spatial variance* σ_X^2:
$$\sigma_X^2 = \langle X^2\rangle - \langle X\rangle^2 \tag{7}$$
- The *temporal variance* σ_t^2 computed from mean values of X at different times, $\bar{X}(t)$, (here we take $\bar{X} \equiv \langle X\rangle(t)$) which is defined as:
$$\sigma_t^2 = \frac{1}{\tau}\sum_{t'=t-\tau}^{t} \bar{X}(t')^2 - \left(\frac{1}{\tau}\sum_{t'=t-\tau}^{t} \bar{X}(t')\right)^2 \tag{8}$$
for temporal bins of size τ (typical values for τ are from 50 to 150).
- The *patchiness* or *cluster structure*. Clusters of high (low) X are defined as connected regions of cells with $X(i,j,t) > X_m$ ($X(i,j,t) < X_m$) where X_m is a threshold value. There are different criteria to define X_m, one of which is stated in section 3.1.
- The *two-point correlation function* for pairs of cells at (i_1, j_1) and (i_2, j_2), separated a given distance R, which is given by:
$$G_2(R) = \langle X(i_1,j_1)X(i_2,j_2)\rangle - \langle X(i_1,i_1)\rangle\langle X(i_2,j_2)\rangle \tag{9}$$

3. Early Warning Signals

We will discuss first the results for the spatial grazing model (q=2 Holling type III consumption) and in a following subsection we do the same for the spatial harvesting model (q=1 Holling type II consumption).

For the grazing model the global parameter c is taken as the *control* parameter, varying with time, representing a changing grazing pressure. For simplicity, is assumed that the the local parameter $K(i,j)$ doesn't change *i.e.* $\langle K\rangle$ = constant = 7.5.

On the other hand, with the harvesting model we illustrate a different situation in which the environmental conditions are changing much more quickly than the consumption rate. For example, sudden droughts or floods can produce drastic modifications of the carrying capacity of a lake. Therefore, we take the global parameter c constant and the local carrying capacity $K(i,j)$ varying with time *i.e.* $\langle K\rangle = \langle K\rangle(t)$.

3.1. Grazing Model

3.1.1. Hysteresis Loops and Spatial Variance Let us start by studying the effect of gradually varying the stress on the system, increasing c from 1 to 3 in 1000 steps (we checked that reducing the number of steps to, for instance, 100 produces only slight quantitative changes). figure 1 shows hysteresis cycles and the spatial variance σ_X^2 for different values of d and $\langle K\rangle = 7.5$ ($X(i,j)$ takes an initial random value in the interval $[0, \langle K\rangle]$ for all cell). Notice that the peak of σ_X^2 occurs always at $c_m \simeq 2.08$ clearly announcing the coming shift. We observe two additional remarkable facts. First, the peak in σ_X^2 is always narrower for the backward transition than in the forward transition. Second, the width of the hysteresis loop and the height of the peak of the variance both decrease with d, this is expected since diffusion tends to mitigate heterogeneities

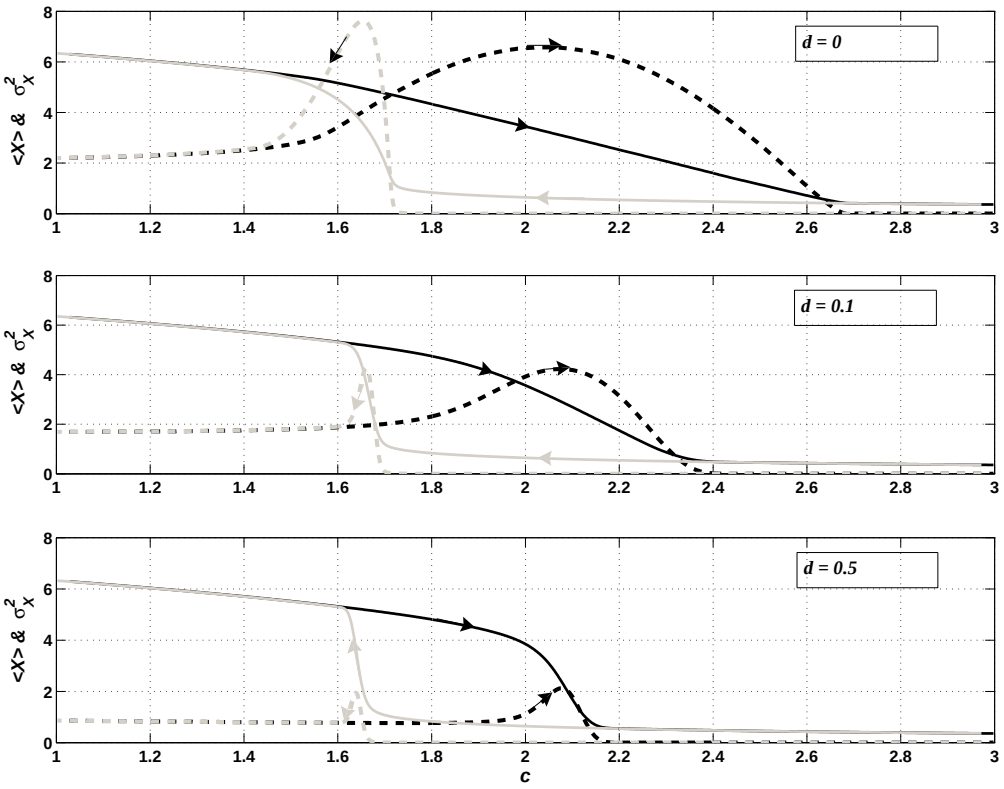

Figure 1. Grazing model: $\langle X\rangle$ (filled curves) and σ_X^2 (dashed curves) for $\langle K\rangle = 7.5$ & $\delta_K = 2.5$, computed for forward (black) and backward (gray) changes of the control parameter c. Results for d=0 (above), d=0.1 (middle) and d=0.5 (below).

3.1.2. Patchiness: Cluster structure In the upper row of figure 2 we show colour maps illustrating the state of the system just at $c = c_m = 2.08$ for d=0.1 and d=0.5. Red (blue) cells correspond to high (low) density of vegetation. As expected, the domain structure becomes more clear as d grows allowing greater segregation.

In order to study the cluster structure we must define a threshold X_m as a reference for the grid values $X(i,j)$. This X_m can be either local, as for example the value of the unstable root that separates the two attractors at each cell, or global e.g. the spatial average of these unstable roots or even the arithmetic mean of both attractors (we checked that these alternative choices do not introduce substantial changes). Thus, cells with X above (below) X_m belong to

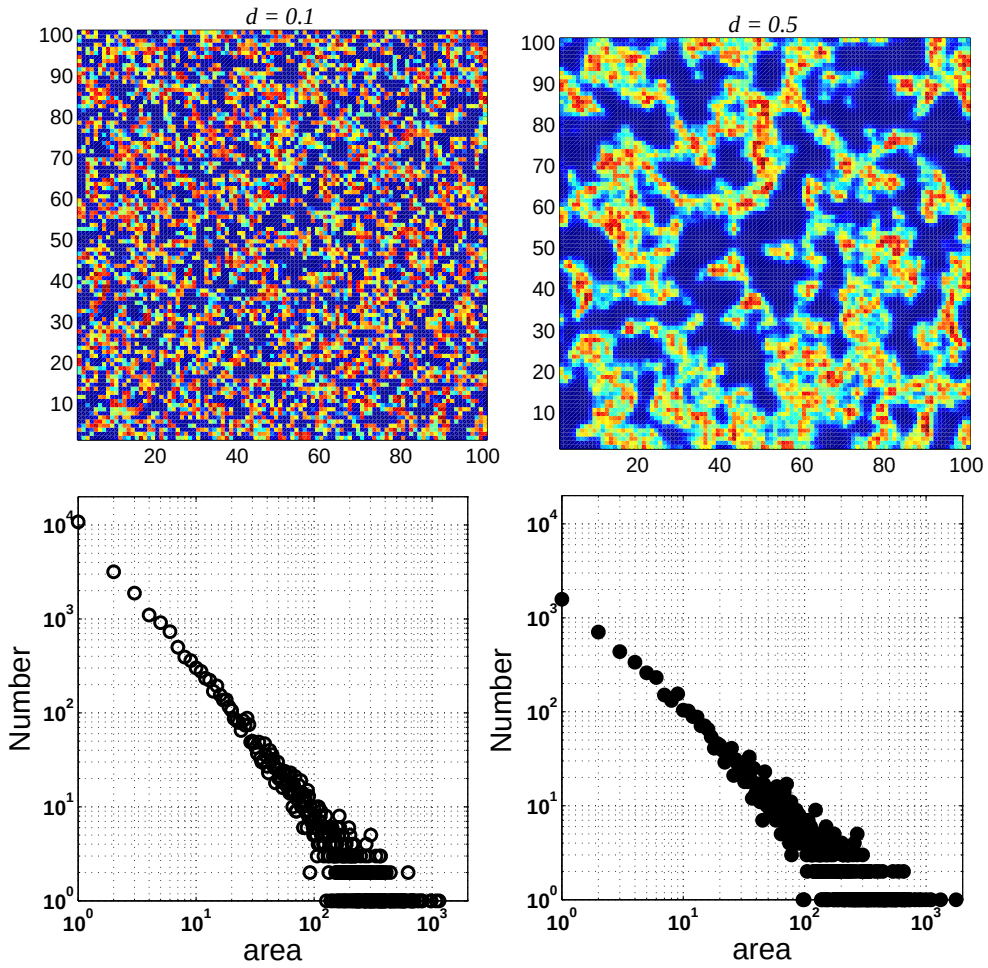

Figure 2. Grazing model: Above: A snapshot at $c = c_m = 2.08$ showing a portion of 100×100 cells, from the original 800×800 lattice, for $\langle K \rangle = 7.5$. Left (right) panel correspond to $d = 0.1$ ($d = 0.5$). Below: The corresponding patch-size distributions measured on the entire 800×800 lattice.

clusters of high (low) concentration of biomass. The value of $\langle X \rangle$ corresponding to $c_m \approx 2.08$ is $\langle X \rangle_{c_m} \approx 2.84$ and we will take it as the threshold. In the lower row of figure 2 we show the corresponding patch-size distributions for d=0.1 and d=0.5. Notice that they follow a power law $N(s) \sim s^{-\gamma}$ over more than two decades, which disappears for smaller or greater values of c e.g. for $c = c_m \pm 0.1$ (not shown). Therefore this particular distribution may be considered as a signature of an upcoming catastrophic shift in the system. It is remarkable that for d=0.5, $\gamma \simeq 1.19$ and thus it is precisely in the range found by Kéfi *et al* for arid Mediterranean ecosystems [16]. Namely between γ=1.06 (for Greece) and $\gamma = 1.23$ (for Spain). For d=0.1 the exponent becomes a little larger, around 1.34.

3.2. Harvesting Model

Variations of the average carrying capacity $\langle K \rangle$ produce hysteresis cycles shown in figure 3 together with the spatial variance σ_X^2 for $d = 0.1$ and c=2.4.

In figure 4 we show, also for $d = 0.1$ and c=2.4, $G_2(R)$ measured over the forward variation

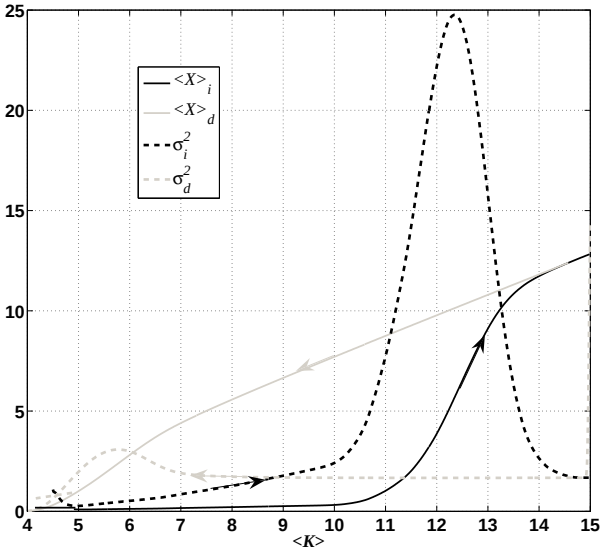

Figure 3. Harvesting model: $\langle X\rangle$ (filled curves) and σ_X^2 (dashed curves) for c =2.4 and d=0.1, computed for forward (black) and backward (gray) changes of the control parameter c.

of $\langle K\rangle$ (from 4.5 to 15) at different values of $\langle K\rangle$. Notice that the correlation increases as the average carrying capacity increases unil the correlation length, ξ, becomes maximum when $\langle K\rangle_m$ = 12.35 (*i.e.* it coincides with the maximum of σ_X^2). It is remarkable that for a wide range of values of $\langle K\rangle$ (relatively far from $\langle K\rangle_m$), the correlation length is greater than 1 lattice spacing (ξ=1.4 for $\langle K\rangle$=10.35).

4. Usefulness of the spatial early warnings

To determine the usefulness of the warning indicators presented in the previous section it is necessary first to assess their practicality and second if they really allow the implementation of corrective actions to avoid the catastrophic shift.

Concerning the question of the practicity of measurements: Calculating variances over grids consisting in a large number of sites (e.g. 400×400 or 800×800) is easy on a computer but involve a formidable task of field data acquisition. So, in order to assess the practical difficulty of estimating σ_X^2, we have performed calculations over sample grids of different sizes $L_s < L$. In figure 5 we show for the grazing model that the signal does not depend qualitatively on the number of points on the grid that are considered to estimate σ_X^2. In fact, even for a very small sample of 9 points, σ_X^2 still exhibits a noticeable peak. Of course, the quality of the signal improves with the size of the sample.

In figure 6 we show spatial variances for the harvesting model computed on 5×5 lattices for forward and backward shifts. Again the signal remains quite clear.

Additionally, since the data from real ecosystems may be very noisy, it is worth considering how the presence of noise alters results. So we assume some level of noise by adding to c a random value belonging to some interval $[-\delta_c, \delta_c]$. In figure 7 we show $\langle X\rangle$ and σ_X^2 for $\delta_c = 0.5$. The rise of σ_X^2 and the anticipation to the temporal variance are still observed.

In relation to possible remedial actions, we will study the consequences of a simple, at least theoretically, corrective measure consisting in immediately stopping the increase of the control parameter after it reaches some threshold value c^*. In figure 8 we show the effect of keeping c

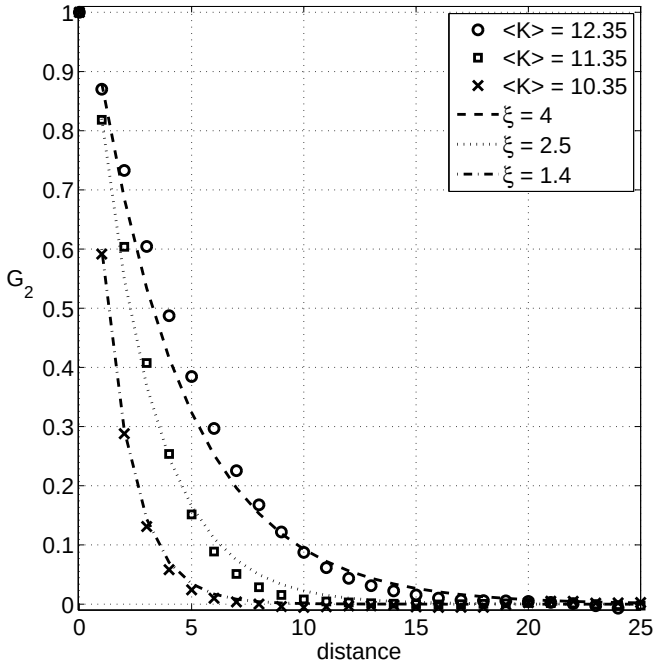

Figure 4. Harvesting model: G_2 vs. the distance R for c =2.4 and d=0.1, computed for forward changes of $\langle K \rangle$ and their corresponding exponential fits $\sim e^{-\xi/R}$.

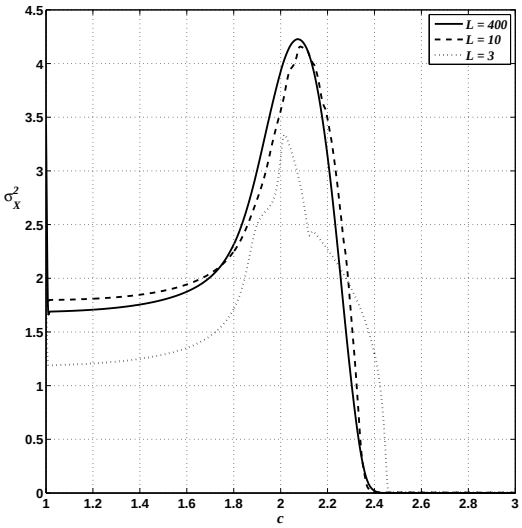

Figure 5. Harvesting model: σ_X^2 for $d = 0.1$, $\langle K \rangle = 7.5$, $\delta_K = 2.5$ calculated on lattices of size L_s=3 (dotted line), L_s=10 and L_s=400 (the entire lattice).

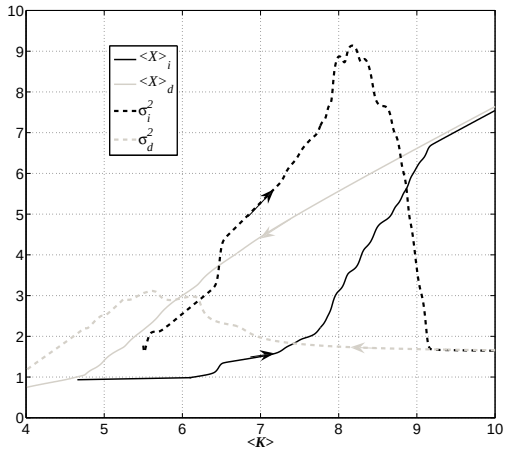

Figure 6. Harvesting model: $\langle X \rangle$ (filled curves) and σ_X^2 (dashed curves) for c =2.4 and d=0.1, computed for forward (black) and backward (gray) changes of the control parameter c for a 5×5 sample lattice.

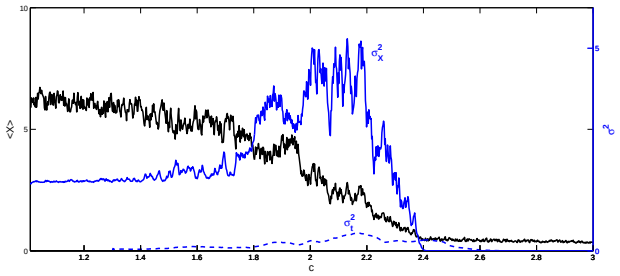

Figure 7. Grazing model: $\langle X \rangle$ (black) and σ_X^2 (blue) for a random noise of amplitude $\delta c = 0.5$.

constant to c^* for different values of c^* and d. For instance, if the measure is applied at the very position of the peak of σ_X^2, $c^* = c_m \simeq 2.08$ ($\langle K \rangle = 7.5$), its usefulness depends on the value of d. For d small ($d = 0.1$) the decay in $\langle X(t) \rangle$ stabilizes soon to a value above 2 *i.e.* the system remains in a mixed state. On the other hand, for larger values of d ($d = 0.5$) the decay in $\langle X(t) \rangle$ continues and the ecosystem passes to the alternative state with low biomass, $\langle X(t) \rangle < 1$. This figure also shows that, for $d = 0.5$, the remedial measure is effective when applied before σ_X^2 reaches its maximum at c_m, for $c^* = 1.9$. We checked that, for moderate or high diffusion (d $\gtrsim$ 0.5), this recipe of management works if c^* is taken between the line corresponding to $\mathcal{S}_M$ and the right fold line of $\mathcal{S}_B$ (closer to the first than to the second one). So a possible criterion to choose c^* is as the points belonging to $\mathcal{S}_M$.

We conclude this section discussing examples of alternative intervention strategies that have been carried out in practice to avoid ASS shifts in different ecosystems as well as potential measures to drive an ecological system back to the original desired ASS.

Fishing pressure is the prime reason that many fish stocks around the world have been strongly reduced [24]. Management has often failed to achieve sustainability. This failure is primarily due to continually increasing harvest rates and the intrinsic uncertainty in predicting the harvest that will cause population collapse. Models suggest that the mechanism of exploitation can by

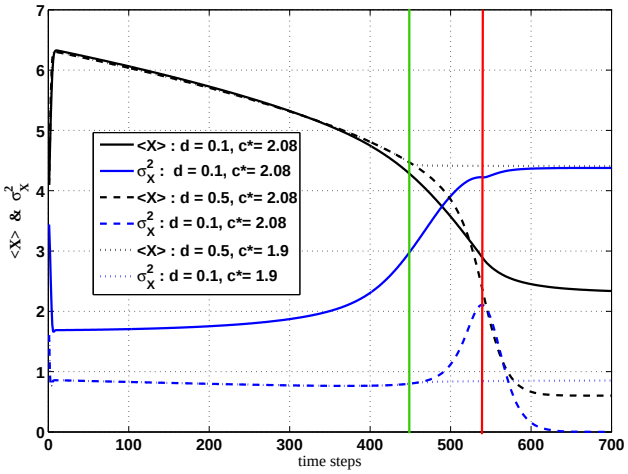

Figure 8. $\langle X\rangle$ (black) and σ_X^2 (blue) for $\langle K\rangle = 7.5$ in the case of a remedial action consisting in keeping constant the control parameter after it reaches some threshold value c^*. The red line indicates a threshold c^* coinciding with the peak of σ_X^2, $c^* = c_m \simeq 2.08$. Full (dashed) curves correspond to d=0.1 (d=0.5). The green line points a value of c^* before c_m, $c^* = 1.9$; in this case we get, for d=0.1, the dotted curves.

itself cause the overexploited state to be an ASS [25]. In that sense, cod populations represent a well-known example of how an economically important fish stock can crash in a dramatic way. However, the lack of recovery decades after the closure of fisheries on Newfoundland cod has raised the question of whether other mechanisms may keep collapsed stocks from recovering. For example, it has been hypothesized that a threshold population of adult stock is needed to control potential predators and competitors of their offspring [26]. Indeed, size structure predator prey interactions may well lead to Allee effects that make it difficult to recover once the population passes this critical threshold [27].

It is interesting that a similar situation occurs for the case of overgrazing in the dry-lands which could cause a stable overexploited state. Some degraded lands did not seem to recover upon removal of the animals, and it was found that an additional positive feedback (between soil condition and vegetation presence) can probably keep the system irreversibly trapped in the degraded state [28].

Another well studied problem is the restoration of non-vegetated turbid shallow lakes to a clear vegetated state (something which sounds good in theory but can be very difficult to achieve in practice). The pristine state of shallow lakes is in general one of clear water and a rich aquatic vegetation, which contribute to preserve this state. Nutrient loading, mainly due to the input of fertilizers from surrounding lands, used for agriculture or farming, has changed this situation in many cases. The increase of nutrients loading rate plays a similar role to the one played by the increase in the consumption rate in harvesting and fisheries, promoting a shift to an undesired ASS. As lakes shift from clear to turbid, submerged plants disappear. A later reduction of the nutrient loading may have little effect in restoring the clear water sate since, during the *eutrophication* enrichment period, a large amount of phosphorus has been absorbed by the sediments. Thus a reduction of the external loading is often compensated by 'internal loading', delaying the response of the lake water concentration to the reduction of external loading. Therefore, in many cases, nutrient reduction alone may be insufficient to restore the clear state in shallow lakes. Additional "indirect" measures such as removal of part of the fish

stock and alteration of the water level have been successfully used as a way to break the feedback that keeps such lakes turbid.

The three examples mentioned demonstrate that the restoration of the original conditions demand strong efforts and often the probability of success can be quite low. An increase of the resilience capacity of ecosystems is the easiest and cheaper way to sustain their critical services like food or water.

5. Analyzing Ecosystem Shifts by using Catastrophe Theory

A general formalism for treating these catastrophic regime shifts in MF is the *Elementary Catastrophe Theory* (ECT) developed by R. Thom [29]. However, ECT works for static and homogeneous (MF) systems, where there is no time or spatial dependence of the potential. To discuss dynamics or local properties, ECT must be extended by incorporating some external assumptions. A change of the control parameter, reflecting changes of the external conditions, modifies the form of the potential. Therefore, as the shape of the potential changes, an original global minimum in which the system sits may become a metastable local minimum because other minimum assumes a lower value, or it even may disappear. In this case the system must jump from the original global minimum to the new one. ECT does not tell us when, and to which minimum, the jump occurs. A criterion to elucidate this is called, in the Catastrophe Theory parlance, a *convention*. The grazing model will serve us to illustrate the effects of the heterogeneity , diffusion and a varying control parameter (c) in modifying the predicitons of ECT.

5.1. Delay vs Maxwell Conventions

The MF 'phase diagram' for the grazing model in the K-c plane is given by the so-called *bifurcation set* $\mathcal{S}_B$ [30]. This is the set of points at which equilibria are either created or destroyed. Therefore it divides the phase space into two regions corresponding either to single stability (one attractor) or bistability (two competing attractors or ASS) (see figure 9). For the (c, K) points on this curve the second derivative of the potential (2) vanishes, so the bifurcation set is given in its parametric form by:

$$c = \frac{(x_1^2+1)^2}{2x_1^3}, \quad K = \frac{2x_1^3}{x_1^2-1} \qquad \text{for } x_1 > 1. \tag{10}$$

$\mathcal{S}_B$ has a cusp point at $c = 8/3^{3/2}$, $K_c = 3^{3/2} \simeq 5.196$. The attractor to the left (right) of $\mathcal{S}_B$ corresponds to high (low) biomass.

Before discussing conventions we need to introduce another important set of points in parameter space which control structural changes of the potential. This second set of points is called the *Maxwell set* $\mathcal{S}_M$ [30]. On $\mathcal{S}_M$ the values of the potential V at two or more stable equilibria are equal. In our case it is defined by:

$$\left(\frac{dV_g}{dX}\right)_{x_1,x_2} = 0 \tag{11}$$

$$V_g(x_1) = V_g(x_2), \tag{12}$$

and is the dashed curve in figure 9.

$\mathcal{S}_B$ and $\mathcal{S}_M$ are connected to two commonly applied criteria or conventions. Systems which remain in the equilibrium that they are in until it disappears are said to obey the *delay* convention. On the other hand, systems which always seek a global minimum of V are said to obey the *Maxwell* convention. Indeed these two conventions correspond to two extremes in a continuum of possibilities. Furthermore, real systems may obey either of these two conventions depending on the rate of change of the control parameters or on other external conditions (see next subsection).

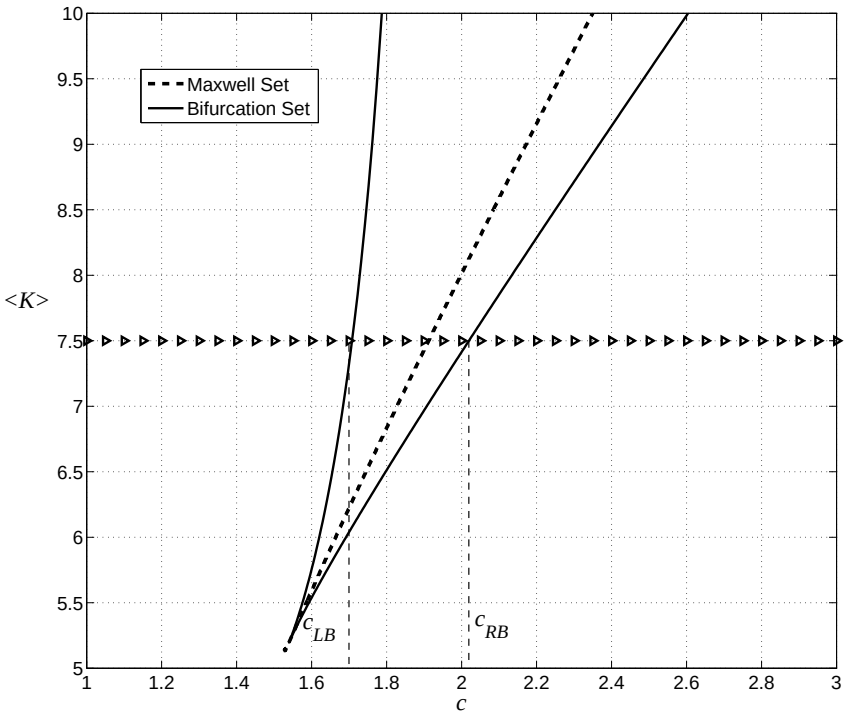

Figure 9. Bifurcation set (solid line) and Maxwell set (dashed) for the grazing model. The line of triangles denote a path at constant $\langle K \rangle = 7.5$, it intersects $\mathcal{S}_B$ at two points c_{LB}=1.7079 and c_{RB}=2.0195.

5.2. The effects of Heterogeneity, Diffusion and Varying Consumption

In our simulations we start from c=1, which is at the left of $\mathcal{S}_B$ *i.e.* with the ecosystem in the upper biomass attractor. Then, increasing the consumption rate c along an horizontal line of constant $\langle K \rangle$ (above K_c) in 1000 time steps $\mathcal{S}_B$ is traversed until c=3, at the right of $\mathcal{S}_B$, where the ecosystem is in the lower biomass attractor.

We found that within the bistability region, under the above conditions, the ecosystem remains always in the upper attractor or very close to it. The transition to the lower attractor occurs for values of c at the right of $\mathcal{S}_B$ and not just over it right component (where the upper attractor disappears). This 'delay' occurs because, since c is increasing, the state of the ecosystem at time t reflects smaller (earlier) values of the control parameter. In other words, in the case of constant c, within the region delimited by $\mathcal{S}_B$ the ecosystem should be in a mixed state and immediately at the right component of $\mathcal{S}_B$ all the ecosystem should be in the lower attractor. In fact we found this is true only when δ_K and d are equal to zero: the spatial heterogeneity together with diffusion modify this.

In order to dissect the effects of the three combined factors -spatial heterogeneity, diffusion and varying consumption rate- we analyze them by separate. That is, we proceed by steps: in the first step we consider the simplest situation, *i.e.* an homogeneous non diffusive and static system, and we add at the other two steps, one by one, the remaining factors. So, starting from a random configuration of $X(i, j)$, depending on the situations listed below, the outcomes within the region delimited by $\mathcal{S}_B$ are as follows.

- *Homogeneous non diffusive and static system i.e.* δ_K=0 (*i.e.* K=7.5 for all cells), d=0 and $dc/dt = 0$: *Bistable state.* In this simplest situation the ecosystems displays a two-colour state. That is, depending if the initial value of X for each cell is above or below the unstable root separating both attractors for the given value of c, this cell adopts respectively the upper or lower attractors. For instance, over the right component of $\mathcal{S}_B$, $c = c_{RB}$, X takes only two values for all the cells: $X_u = 3.455$ (upper attractor) or $X_l = 0.637$ (lower attractor), as shown in figure 10-A. Just at the right of this curve, $c = c_{RB}^{+}$, the whole ecosystem collapses to its lower attractor.

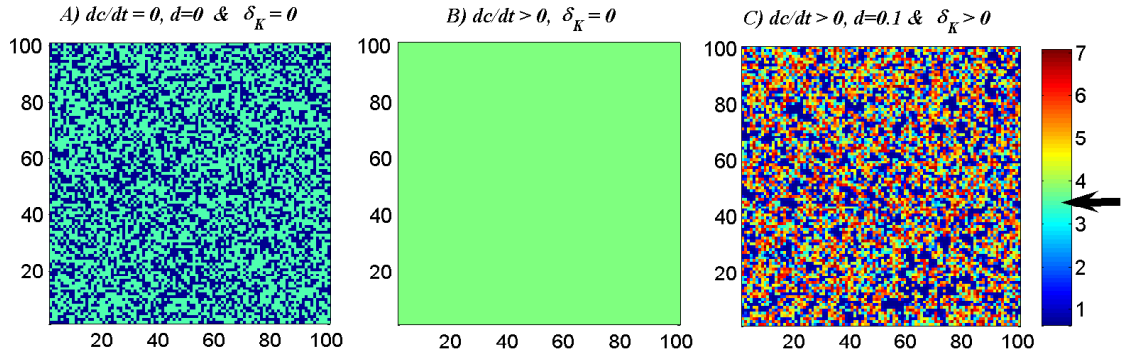

Figure 10. Snapshots at $c = c_{RB}$ showing a portion of 100×100 cells, from the original 800×800 lattice, for the three different situations listed in the text. The black arrow points to the value of the upper attractor at $c = c_{RB}$: X_u=3.455.

- *Dynamic but homogeneous system i.e.* δ_K=0, either with d=0 or $d > 0$, and $dc/dt > 0$: *Homogeneous state (upper attractor).* Now, the point representing the system in figure 9 starts at the single upper attractor region $c < c_{LB}$. As c increases, the ecosystem quickly adopts an homogeneous state coinciding with the corresponding upper attractor. When it enters the region delimited by $\mathcal{S}_B$ it "keeps memory" and remains in the upper attractor state. In figure 10-B it is shown this for $c = c_{RB}$ for which the whole ecosystem adopted a state of $X(i,j) \simeq 3.816\ \forall(i,j)$ which is slightly higher than X_u. This small difference is explained by the reaction delay mentioned above (*i.e.* if c is freezed to c_{RB} all the cells converge to X_u). The homogeneity of the state persists even after the ecosystem traversed the entire region delimited by $\mathcal{S}_B$ and the transition to the lower attractor occurs for $c > c_{RB}$ in a quite gradual and soft way.

- *Heterogeneous diffusive dynamic system i.e.* $\delta_K > 0$, $d > 0$, $dc/dt > 0$: *Quasi upper attractor.* In this ordinary situation, the underlying heterogeneity of the environment leads to an heterogeneous state. However, at least on average, this state is much more closer to the upper attractor than to the lower one: for $c = c_{RB}$ $\langle X(i,j)\rangle \simeq 3.41$ which is slightly lower than X_u, the value of the corresponding upper attractor (see figure 10-C).

5.3. Comparison between Shifts in Ecosystems and the Phenomenology of Thermodynamic Phase Transitions

Some of the characteristic fingerprints or 'wave flags' for catastrophes are: *modality, sudden jumps, hysteresis* and a *large* or *anomalous variance* [30]. These are precisely the signals we found for the considered spatial heterogeneous ecological models representing a species or set of species subject to exploitation (either grazing or harvesting).

It is interesting to analyze similarities and differences with the liquid-vapour transition in a fluid, like water. Therefore, the biomass density X would correspond to the fluid density, the liquid to the high biomass density attractor and the vapour to the low biomass density attractor. Let us compare the above catastrophe flags for the fluid vs. the ecosystem:

- Modality: The fluid is bimodal in the neighbourhood of the liquid-gas coexistence curve, having well defined liquid and gas states (bubbles in liquid or droplets in vapour). So this is similar in both systems.

- Sudden Jumps: In the case of the fluid it is certainly true that sudden jumps occur, since there is an abrupt increase in volume when a liquid transforms into vapour. However, this large change in volume occurs when a slight change in the temperature and pressure moves the fluid from one side of the coexistence curve to the other. Hence, the liquid-vapour coexistence curve can be identified with $\mathcal{S}_M$ and the water changes of state obey in general the Maxwell convention.
  On the other hand, the shift in the considered model always obeys the delay convention: the ecosystem remains in the higher attractor (higher values of X) until the bifurcation set is completely traversed. However, when perturbations are big enough they can allow the switching between equilibria on different stability branches, the systems may follow the Maxwell convention. We have checked that the effect of a sudden perturbation of the environment, represented for example by a sharp decrease of the average carrying capacity $\langle K\rangle$ followed by a slow recovery, produces a change of convention: from delay to Maxwell [31].

- Hysteresis: In everyday situations one does not observe hysteresis in the liquid-gas phase transition of water: the liquid usually boils at the same temperature at which the vapour condenses. In other words, water changes of state obey in general the Maxwell convention. Nevertheless, a careful experimentalist can obtain an hysteresis cycle by first raising the temperature and superheating the liquid, and after evaporation, cooling the gas below the condensation point. Indeed the coexistence curve is surrounded by two *spinodal lines* which determine the limits to superheating and supersaturation. These spinodal or fold lines can then be identified with $\mathcal{S}_B$.

- Anomalous Variance: When a fluid condenses (boils) from its gas (liquid) to its liquid (gas) state, small droplets (bubbles) are formed. As a consequence, the variance of the volume may become large, similarly to what happens for the ecosystem.

6. Acknowledgments

H. F. and N. M. acknowledge support from Project PDT 63/13 and PEDECIBA-Uruguay and from ANII.

References

[1] L J McCook. Macroalgae, nutrients and phase shifts on coral reefs: scientific issues and management consequences for the great barrier reef. *Coral Reef*, 18:357, 1999.
[2] M Nystrom et al. Coral reef disturbance and resilience in a human-dominated environment. *Trends Ecol. Evol.*, 15:413, 2000.
[3] M Scheffer et al. Floating plant dominance as a stable state. *Proc. Natl. Acad. Sci. USA*, 100:4040, 2003.
[4] D Ludwig et al. Sustainability, stability, and resilience. *Conserv. Ecol.*, 1:http://www.consecol.org/vol1/iss1/art7, 1997.
[5] B H Walker. Rangeland ecology: understanding and managing change. *Ambio*, 22:2, 1993.
[6] M Scheffer. *Ecology of Shallow Lakes*. Chapman & Hall, 1998.
[7] S R Carpenter et al. Management of eutrophication for lakes subject to potentially irreversible change. *Ecol. Appl.*, 9:751, 1999.
[8] M Scheffer et al. Catastrophic shifts in ecosystems. *Nature*, 413:591, 2001.
[9] S Carpenter. Alternate states of ecosystems: evidence and some implications. In Huntly N. Press, M. C. and S. Levin, editors, *Ecology: achievement and challenge*, pages 357–381. Blackwell, London, UK, 2001.
[10] E K Steinberg and P Kareiva. Challenges and opportunities for empirical evaluation of spatial theory. In D. Tilman and P. Kareiva, editors, *Ecology: achievement and challenge*, pages 318–332. Princeton University, 1997.
[11] S A Levin and S W Pacala. Theories of simplification and scaling of spatially distributed processes. In D. Tilman and P. Kareiva, editors, *Ecology: achievement and challenge*, pages 271–296. Princeton University, 1997.
[12] M R Aguiar and O E Sala. Patch structure, dynamics and implications for the functioning of arid ecosystems. *Tree*, 14:273, 1999.
[13] C A Klausmeier. Regular and irregular patterns in semiarid vegetation. *Science*, 284:1826, 1999.
[14] J. von andd others Hardenberg. Diversity of vegetation patterns and desertification. *Phys. Rev. Lett.*, 87:1981011, 2001.
[15] M Rietkerk et al. Self-organized patchiness and catastrophic shifts in ecosystems. *Science*, 305:1926, 2004.
[16] S Kéfi et al. Spatial vegetation patterns and imminent desertification in mediterranean arid ecosystems. *Nature*, 449:213, 2007.
[17] S R Carpenter and W A Brock. Rising variance: a leading indicator of ecological transition. *Ecology Letters*, 9:311, 2006.
[18] C S Holling. The components of predation as revealed by a study of small mammal predation of the european pine sawfly. *Canadian Entomol.*, 91:293, 1959.
[19] I Noy-Meir. Stability of grazing systems: an application of predator-prey graphs. *Jour. of Ecology*, 63:459, 1975.
[20] R M May. Thresholds and breakpoints in ecosystems with a multiplicity of stable states. *Nature*, 269:471, 1977.
[21] D Ludwig, D D Jones, and C S Holling. Qualitative analysis of insect outbreak systems: the spruce budworm and forest. *Jour. Anim. Ecology*, 47:315, 1978.
[22] J D Murray. *Mathematical Biology*. Springer-Verlag, 1993.
[23] E van Nes, van den Bergb M S Scheffer, M, and H Coops. Aquatic macrophytes: restore, eradicate or is there a compromise? *Aquatic Botany*, 72:387, 2002.
[24] L W Botsford et al. The management of fisheries and marine ecosystems. *Science*, 277:509, 1997.
[25] J H Steele and Henderson E W. Modeling long-term fluctuations in fish stocks. *Science*, 224:985, 1984.
[26] C J Walters and J F Kitchell. Cultivation/depensation effects on juvenile survival and recruitment. *Aquat. Sci.*, 58:39, 2002.
[27] M. Scheffer. *Critical Transitions in Nature and Society*. Princeton University Press, 2009.
[28] M. Rietkerk and J Van de Koppel. Alternate stable states and threshold effects in semi-arid grazing systems. *Oikos*, 79:69, 1997.
[29] R Thom. *Structural Stability and Morphogenesis*. Reading: Benjamin, 1975.
[30] R Gilmore. *Catastrophe Theory for Scientists and Engineers*. Dover, 1981.
[31] A Fernandez and H Fort. Early warnings of catastrophic shifts in ecosystems: Comparison between spatial and temporal indicators. *J. Stat. Mech.*, P09014:1–17, 2009.